



Three Dimensional View of Radial Profile of Fe XV at Particular Electron Temperature at the Axis of Tokamak for Better Understanding of Radial Distribution of Fractional Abundance in Tokamak Plasma



A. N. Jadhav¹

¹ Department of Electronics, Yeshwant Mahavidyalaya, Nanded
Affiliated to Swami Ramanand Teerth Marathwada, University, Nanded
(Maharashtra)

Email: angadjadhav2007@rediffmail.com

Abstract

Parameters of tokamak plasma like electron temperature, fractional abundance etc do not have uniform values across the plasma column in the tokamak discharge. The Fractional Abundance of impurity ions like *Fe XV* in the tokamak plasma is mainly determined by electron temperature. In this work, various rate coefficients at a particular electron temperature at the axis are determined to compute Fractional Abundance which is a function of electron temperature and radial distance from the axis of plasma column to wall of tokamak. The Radial Profile of fractional Abundance of *Fe XV* at a particular Electron temperature at the axis of tokamak is studied by considering three dimensional view.

Keywords: Tokamak plasma, Electron Temperature, Rate Coefficients, Fractional Abundance, Radial Profile.

Subject Classification: Plasma

1. Introduction

A tokamak is an axisymmetrical toroidal system in which a hot and rather dense hydrogen or deuterium plasma is confined within a poloidal magnetic field B_p created by the current I_p flowing through it (typical values are $I_p= 100$ to 1000 kA and $B_p=1$ to 5 kG). The plasma column remains stable against magnetohydrodynamic motions provided by strong toroidal magnetic field, depending on the type of tokamak and operating conditions exists within the plasma. The magnetic-field lines formed by the superposition of poloidal and toroidal fields are helices which revolve around a toroidal axis on surfaces called as magnetic surfaces,



confining the plasma ions and electrons by forcing them to move along helical orbits around the field lines [1].

2. Impurity Production in Tokamak

Besides the basic gas ions (generally protons and deuterons), tokamak plasmas always contain tresses of impurity ions, produced by interaction with limiter and /or the liner, such interactive ions are generally referred to as plasma- wall interaction phenomena [2].

The observed impurity elements (elements as heavy as tungsten and gold have been detected) can be broadly divided into two classes, according to the mechanism responsible for their production at the walls and / or the limiter i.e. desorbed and eroded impurities. This is better characterization than the customary division between light impurities, which are completely stripped in the centre of tokamak discharges and which therefore do not emit central line radiation and heavy impurities which can only be partly stripped in these plasmas since the ionisation potential αz of their last hydrogen like ion is much higher than the central electron temperature.

On the basis of this differentiation, nitrogen, oxygen and chlorine are the most frequently observed desorbed elements and the metallic components of the limiters and / or the walls, essentially Ti, Fe, Cr and Ni in most tokamaks are eroded impurities. The principal processes by which the wall material can be removed are sputtering, unipolar arcs and evaporation.

An impurity atom is ionized by electron impact to successively higher charge states as it penetrates progressively into the discharge where it finds an increasing electron temperature. The radial velocity of this movement perpendicular to the field lines is much smaller (typically 10^3 cm/sec) than the thermal velocity of the unimpeded movement along the magnetic field lines (having typical values greater than 10^5 cm/sec), which leads rapidly to a uniform spread over the magnetic surfaces. Because of this reason the impurity ion emission is generally uniform around the torus.

3. Effects of Impurity Production On Tokamak Efficiency

The impurities have profound effects, some deleterious and some beneficial. One of the most important effects of impurities is their contribution to the energy balance through their radiation losses, particularly due to heavy impurities. Because they are incompletely stripped over the entire plasma and radiate strongly. As the impurity increases, there is a point at which all the input power will be radiated away.

Light impurities are not necessarily bad for the plasma, because they help to



evacuate the heat to the walls and keep down the peripheral temperature. However, when attempting to increase N_e to its maximum possible value, light impurity radiation increases eventually leading to a major plasma disruption [3-5]

The effect of heavy impurities, such as iron, nickel, etc (metals characteristic of the wall and limiter) is significantly different from that of light impurities. A major difference is that unlike light impurities, heavy elements are not fully stripped in the centre of the discharge and therefore can contribute significantly to the discharge power balance by line radiation. If proper care is not taken in keeping heavy impurity concentrations low, the central power balance can be dominated by heavy impurity. Line radiation, eventually leading to hollow T_e profiles [6], moreover, even a small amount of heavy impurities can prevent tokamak ignition by too large line radiation losses.

4. Radial Profile of Electron Temperature

In studying the radial profiles of the spectral emission from the plasma, the variation of temperature across the plasma cross section plays vital role. Therefore, an appropriate temperature profile has to be considered.

Fractional abundance of impurity ions in the plasma is mainly determined by the electron temperature. As we know that the temperature at the torus axis is maximum and it goes on decreasing towards the wall. Thus, the suitable radial profile which would fulfill the above said boundary conditions must be assumed. The profile of electron temperature across the plasma can be considered to be of two types which are given by following equations.

$$T(R) = T_0 [1 - (R/R_0)^2] \quad (1)$$

$$T(R) = T_0 [1 - (R/R_0)]^2 \quad (2)$$

Where T_0 is axial temperature.

R is radial distance at a point in the torus.

R_0 is radius of cross section of plasma column

These two radial profiles are shown in figure (1). In the first profile (dotted curve) the temperature decline is slow as one goes from axis to the walls. The second profile (solid curve) shows fast decline of temperature as one goes from axis towards the walls. Usually first profile is considered suitable because it shows similarity with the Maxwellian distribution function. This nature of profile is in close agreement with the nature of graph plotted by TFR group [7].

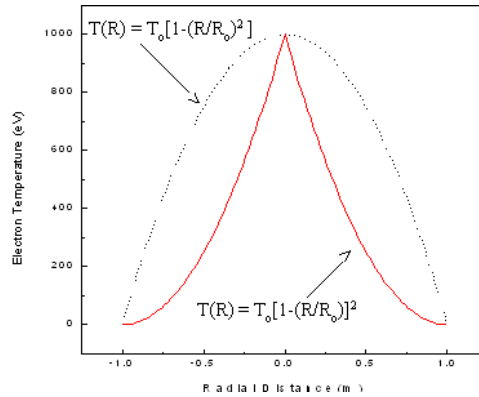


Fig.1 Radial profile of Electron Temperature (T_e) in Tokamak Plasma at 1000 eV

5. Rate Coefficients

To study Radial profile of Fractional Abundance of Fe XV at a particular Temperature at the axis of tokamak, following rate coefficients are computed to determine fractional abundance as a function of electron temperature.

5.1 Ionization Rate Coefficient (S_z)

The Ionization Rate Coefficient of Fe XV computed using Lotz Formula [8] by considering contribution of last three subshells.

$$S_z(T_e) = 6.7 \times 10^7 \sum_{i=1}^N \frac{a_i \xi_i}{(T_e)^{3/2}} \left\{ \frac{E_1(X)}{(I_{zi}/T_e)} - \frac{b_i \text{EXP}(e_i)}{(I_{zi}/T_e) + e_i} E1(Y) \right\} \quad (3)$$

where, S_z is the ionization rate coefficient in cm^3 / Sec .

T_e is the electron temperature in eV.

I_{zi} is the ionization energy in eV of the electrons in i^{th} subshell of the ions of charge z .

α_i is the number of equivalent electrons in the i^{th} subshell.

a_i , b_i and c_i are constants for highly ionized ions, Lotz proposed $a_i = 4.5 \times 10^{-14} \text{ cm}^2 \text{ eV}^2$,

$b_i = c_i = 0$. The terms $\alpha_1(X)$ and $E1(Y)$ are exponential integral functions.

Where $X = (I_{zi}/T_e)$ and $Y = (I_{zi}/T_e) + c_i$

Where $E_1(X) = \int_x^\infty X^{-1} e^{-x} dx$ and $E_1(Y) = \int_x^\infty Y^{-1} e^{-y} dY$

where N the number of subshells contributing to the ionization.



Lotz proposed that $N = 1$ for H and He - like ions, $N = 2$ for isoelectronic sequences from Li to Ne and $N = 3$ for isoelectronic sequences from Na to Zn and onwards.

5.2 Excitation Autoionization Rate Coefficient $C_{EA}(T_e)$

To compute Excitation Autoionization rate coefficient, formula adopted by Arnaud and J. Raymond [9] is considered.

$$C_{EA}(T_e) = \frac{6.69 \times 10^7 \times e^{-x}}{(KT_e)^{1/2}} \times F(x) \quad \text{cm}^3 \text{sec}^{-1}$$

$$F(x) = A+B[1-x f_1(x)] + C [1-x\{1-x f_1(x)\}] \\ + D[1-0.5\{x-x^2 + x^3 f_1(x)\}] + E f_1(x)$$

$$\text{Where } x = (I_{EA}/KT_e) \quad \text{and} \quad f_1(x) = e^x \int_0^{\infty} (1/t) e^{-tx} dt$$

where KT_e and I_{EA} are in eV.

where for Fe XV, the values of the constants A, B, C, D and E are, respectively 0, 0, 0, $4.81 \times 10^{-16} \text{ cm}^2 \text{ eV}$.

IEA is the excitation autoionization threshold.

6. Dielectronic Recombination Rate Coefficient

To compute Dielectronic Recombination Rate Coefficient, the expressions used by Burgess (1965) [10]

$$B(z) = 6.5 \times 10^{-10} \times \frac{z^{1/2} (z+1)^2}{(z^2 + 13.4)^{1/2}}$$

$$A(z,j) = \frac{F_{zj} (E_{zj})^{1/2}}{(1 + 0.105 \chi_{zj} + 0.015 \chi_{zj}^2)}$$

where F_{zj} is the absorption oscillator strength of resonant transition j of the ion of charge z and χ_{zj} is given by the equation,

$$\chi_{zj} = \frac{E_{zj}}{(z+1) I_H}$$

6.1 Radiative Recombination Rate Coefficient

The formula which may be used for computation of Radiative Recombination Rate Coefficient $\alpha(rz)$ in the plasma [11] is expressed as,

$$\alpha_{rz} = 2.6 \times 10^{-14} (\alpha_1 + \alpha_2) \text{ cm}^3 \text{ sec}^{-1}$$

Where α_1 & α_2 are expressed as,

$$\alpha_1 = z^2 (I_H / T_e)^{1/2} \times (\mu / n^3) \times (I_{z-1} / t_e) \times e^{(I_{z-1} / T_e)} \times E_1(X_1)$$

$$\alpha_2 = \sum_{\nu=1}^{\infty} 2 \{ z^4 / (n + \nu)^3 \} \times (I_H / T_e)^{3/2} \times \text{EXP}[z^2 I_H / \{(n + \nu)^2 T_e\}] \times E_1(Y_1) \text{ Where,}$$

$$E_1(X_1) = \int_{X_1}^{\infty} X_1^{-1} e^{-X_1} \quad \& \quad E_1(Y_1) = \int_{Y_1}^{\infty} Y_1^{-1} e^{-Y_1}$$

Where $X_1 = I_{z-1} / T_e$ and $Y_1 = z^2 I_H / \{(n + \nu)^2 T_e\}$

where α_{rz}

is the radioactive recombination rate coefficient of an ion of charge Z in $\text{cm}^3 \text{ sec}^{-1}$.

$I_H = 13.6 \text{ eV}$ is ionization potential of hydrogen atom.

α_1 is the contribution from the valance shell (of principle quantum number n) which is partially filled.

α_2 represents the recombination in the excess levels which are considered to be hydrogenic.

α is the number of empty places in valance shell (there are $2n^2$ places in an empty shell).

p is the number of equivalent electrons in the shell.

I_{z-1} is the ionization potential of the ion after recombination.

$E_1(X_1)$ and $E_1(Y_1)$ are the exponential integral functions.

n is the principal quantum number.

The number of empty places (a) may be obtained from the principal quantum number and the number of equivalent electrons (p) in the shell, using the equation, $\alpha = (2n^2 - p)$

7. Fractional Abundance

Plasma consists of the electrons and the ions with different charges. The collision between the atoms, ions of different charges and electrons results in ionization. At the same time the ions may capture the electrons and results in formation of ions of lower charge. The ionization and Recombination processes compete each other so that the ionization rate and recombination rate reach, each to a certain value and equilibrium is attained. As long as the electron temperature is not changed the equilibrium remains in a particular state. A change in electron temperature results in changing the densities of ions and electrons. Thus densities of ions and electrons are completely dictated by the electron temperature. The plasma emission depends upon the fraction of total density of species remaining in a particular ionized state, the electron density and the electron temperature.

The amount of the fraction of the total density of species remaining in a particular ionized state is called as fractional abundance of that ion.

Equation for the time rate of change of population density of ion of charge z can be written as,

$$\frac{dN_z}{dt} = n_e \{ -N_z S_z + N_{z-1} S_{z-1} - N_z \alpha_z + N_{z+1} \alpha_{z+1} \} \quad (4)$$

where z takes all values between 0 and maximum charge on the ion.

The ionization state of each element of atomic number z is controlled by electron impact ionization (including autoionization) from state $z \rightarrow z + 1$ with total rate coefficient $S_{z,z}$ ($\text{cm}^3 \text{sec}^{-1}$) and radiative plus dielectronic recombination $z+1 \rightarrow z$ with rate coefficient $\alpha_{z,z+1}$ ($\text{cm}^3 \text{sec}^{-1}$)

In steady state, the time rate of change of population density of ion of charge z will be zero. In steady state condition, where the time rate change of population density of ion of charge z will be zero, the equation (4) reduces to,

$$N_z \alpha_z = N_{z+1} \alpha_{z+1}$$

The population density ratio ($N_{z,z+1}/N_{z,z}$) of two adjacent ion stages $Z^{+(z+1)}$ and Z^{+z} can be derived from above steady state equation as,

$$\frac{N_{z+1}}{N_z} = \frac{S_z}{\alpha_{z+1}} \quad (5)$$

where $S_{(z)}$ is ionization rate coefficient of ion of charge z . α_{z+1} is recombination rate coefficient of ion of charge $z+1$. N_z and N_{z+1} are densities of ion with charge z and $z+1$ respectively.

7.1 Expression for Fractional Abundance

Thus, population density ratio ($N_{z,z+1} / N_{z,z}$) can be evaluated in terms of S_z and α_{z+1} . As the values of S_z and α_{z+1} are fully determined by the electron temperature. Therefore the fractional abundance and population density of any ion in the plasma depends only on the electron temperature [8]. The fractional abundance of a Fe XV species in the tokamak plasma is evaluated by using equation (5) and the procedure followed by [12] is considered to get formula for Fractional abundance.



The fractional abundance of an ion of charge z can be written as,

$$F_z = \frac{N_z}{\sum_{z'} N_{z'}} \quad (6)$$

where F_z , the fractional abundance of ion of charge z . N_z , the density of ion with charge z . The sum runs over all possible ionized states

8. Results and Discussion

The behavior of fractional abundance may be very well understood from the study of three dimensional plots of fractional abundance.

Typical three dimensional plots of the spatial distribution of *Fe XV* ions for axial electron temperatures 225 eV, 300 eV, 400 eV and 600 eV are shown in figure (2) to figure (5). The figures give very well feeling about the spatial distribution of fractional abundances of the ionic species. Let's suppose that the electron temperature at which fractional abundance is maximum is T_p . If electron temperature is greater than the electron temperature T_p , corresponding to maximum fractional abundance, the plot of the Radial profile shows a well shaped structure as shown in figure (2). Whereas if the temperature on the axis is less than T_p , the Radial profile show hill shaped structure. If the electron temperature on the axis is increased further beyond T_p , the rim of the well goes on shifting towards the wall and the depth of the well goes on increasing as shown in figure (3) and figure (4).

Another three dimensional view of same ion with axial electron temperature 600 eV is shown in figure (5). From these plots of Radial profile, it is observed that the region of maximum fractional abundance shifts towards the wall. Thus, we may say that if the axial electron temperature exceeds the electron temperature T_p corresponding to the maximum fractional abundance of the ion, and if it increases to higher values, the region of maximum fractional abundance of that ion shifts towards walls of the tokamak compared to that having axial electron temperature 400 eV in figure (4).

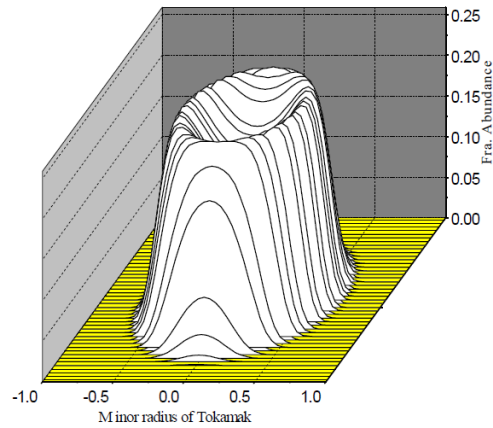


Fig. 2 Three Dimensional View of Radial Profile Of Fe XV When Electron Temperature At The Axis Of Tokamak Is 225 eV.

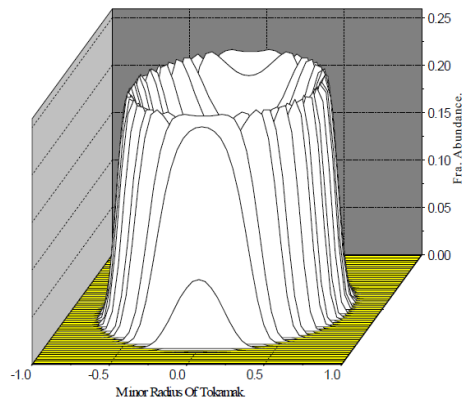


Fig. 3 Three Dimensional View Of Radial Profile Of Fe XV When Electron Temperature At The Axis Of Tokamak Is 300 eV.

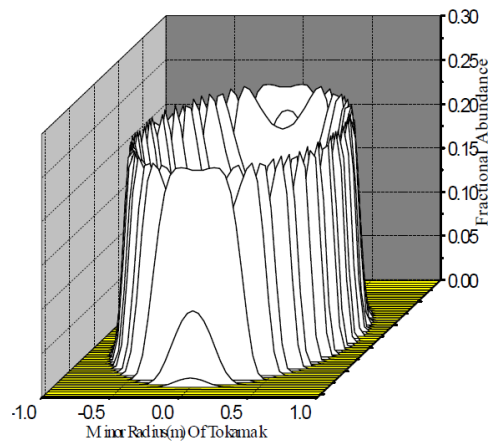


Fig. 4 Three Dimensional View Of Radial Profile Of Fe XV When Electron Temperature At The Axis Of Tokamak Is 400 eV.

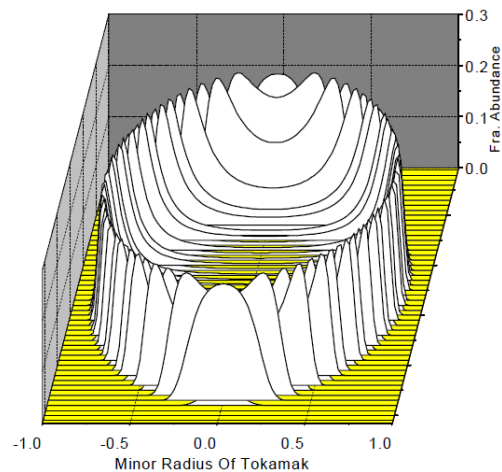


Fig. 5 Three Dimensional View Of Radial Profile Of Fe XV When Electron Temperature At The Axis Of Tokamak Is 600 eV.

9. Conclusion

- 1) If the temperature on the axis is less than T_p corresponding to maximum fractional abundance, the Radial profile show hill shaped structure.
- 2) If electron temperature is greater than the electron temperature T_p , corresponding to maximum fractional abundance, the plot of the Radial profile shows a well shaped structure.
- 3) If the electron temperature on the axis is increased further beyond T_p , the rim of the well goes on shifting towards the wall and the depth of the well goes on increasing.

7. References

- [1] De Michelis, C. and Aattioli, M., Rep. Prog. Phys. 47, 1233-1346 (1984)
- [2] Mc Crackan G. M. & Stott, P. E., Nucl. Fusion, 19, 889-981, (1979).
- [3] Meisel, D. et al, Proc. 6th Int. Conf. On plasma Physics and controlled Nuclear Fusion Research, Berchtesgaden, 1976 Vol. 1 (Vienna : IAEA) pp 259-64, (1977)
- [4] Equipe TFR, Nucl. Fusion, 17, 1283-96, (1977a)
- [5] Toi, K., Itoh, S., Kadota, K., Kawahata, K, Noda N., Sakurai, K., Sato, K., Tanqhashi, S. and Yasue, S. Nucl. Fusion, 19, 1643-63, (1976)
- [6] Hawryluk, R. J. et al, Nucl. Fusion 19, 1307-17, (1979b).



-
-
- [7] TFR group, Plasma Physics, Vol.19, pp-349 -361
- [8] W. Lotz Repts IPP 1/62 and 1/76 Graching Plasma physica institute, Graching bei Munchen federal Republic of Germany, (1967) and (1988).
- [9] N. Arnaud and J. Raymond, The Astrophysical Journal 398: 394-406, Oct, 10, 1992.
- [10] A. Burgess, Astrophys J, Vol. 141, pp 1588, (1965)
- [11] C. Breton, C. Demichelis and M. Mattioli J. Quantitative Spectroscopy and Radiative Transfer, Vol.19, pp 367, (1978)
- [12] A N Jadhav, *Fractional abundance of neutral atoms and ionic species of iron and molybdenum as a function of electron temperature in astrophysical and laboratory plasma*, IJARBAS, Vol.2 Issue 1, pp 12, (2015).